Journal of Geodesy (2003) 77: 465–477
DOI 10.1007/s00190-003-0349-y

Journal of Geodesy

Computation of spherical harmonic coefficients from gravity gradiometry data to be acquired by the GOCE satellite: regularization issues

P. Ditmar, J. Kusche, R. Klees

Physical, Geometrical and Space Geodesy (FMR), Faculty of Civil Engineering and Geosciences, Delft University of Technology, Thijsseweg 11, 2629 JA Delft, The Netherlands; e-mail: ditmar@citg.tudelft.nl; Tel.: +31-15-2782501; Fax: +31-15-2783711

Received: 29 October 2002 / Accepted: 1 July 2003

Abstract. The issue of optimal regularization is investigated in the context of the processing of satellite gravity gradiometry (SGG) data that will be acquired by the GOCE (Gravity Field and Steady-State Ocean Circulation Explorer) satellite. These data are considered as the input for determination of the Earth's gravity field in the form of a series of spherical harmonics. Exploitation of a recently developed fast processing algorithm allowed a very realistic setup of the numerical experiments to be specified, in particular: a non-repeat orbit; 1-s sampling rate; half-year duration of data series; and maximum degree and order set to 300. The first goal of the study is to compare different regularization techniques (regularization matrices). The conclusion is that the first-order Tikhonov regularization matrix (the elements are practically proportional to the degree squared) and the Kaula regularization matrix (the elements are proportional to the fourth power of the degree) are somewhat superior to other regularization techniques. The second goal is to assess the generalized cross-validation method for the selection of the regularization parameter. The inference is that the regularization parameter found this way is very reasonable. The time expenditure required by the generalized cross-validation method remains modest even when a half-year set of SGG data is considered. The numerical study also allows conclusions to be drawn regarding the quality of the Earth's gravity field model that can be obtained from the GOCE SGG data. In particular, it is shown that the cumulative geoid height error between degrees 31 and 200 will not exceed 1 cm.

Keywords: Earth's gravity field – Satellite gravity gradiometry – Gravity Field and Steady-State Ocean Circulation Explorer (GOCE) – Regularization – Generalized cross-validation

Correspondence to: P. Ditmar

1 Introduction

GOCE (Gravity Field and Steady-State Ocean Circulation Explorer) is a satellite mission to be launched in 2006 within the ESA's Earth Explorer program [European Space Agency (ESA) 1999]. The aim of the mission is to provide a high-accuracy, high-resolution model of the Earth's static gravity field and of the geoid. The mission will last for 20 months, including two 6-month observation periods. The satellite orbit will be almost circular, with an average elevation above the equator between 250 and 270 km. The orbit inclination will be about 96.6 degrees, so that the polar areas of the Earth will not be covered by observations. Therefore, any gravity field model produced from GOCE data only will suffer from polar gaps. The satellite will be supplied with a drag-free control system to compensate for non-gravitational forces like the atmospheric drag. A GPS receiver on board will provide the data for a precise orbit determination. Two types of data will be exploited for gravity field determination: (1) GPS measurements (high–low satellite-to-satellite tracking data) and (2) satellite gravity gradiometry (SGG) data. This paper refers only to the latter type of data. The gravity gradiometer on board the GOCE satellite will measure the second-order derivatives of the gravitational potential (or, for brevity, the gravity gradients tensor). It is planned that four components of the gravity gradients tensor will be recorded with high accuracy for the purpose of further processing: XX, YY, ZZ, and XZ (the X-axis is directed along the track, the Y-axis coincides with the direction of the orbital angular momentum, and the Z-axis completes the frame to a right-handed one). The sampling rate will be 1 s. Thus, the total number of collected SGG data will be of the order of 100 million.

A commonly used procedure to represent the Earth's gravity field is the series expansion into spherical harmonics. Although we may describe in this way the gravity field in the whole three-dimensional

(3-D) space above the surface, most of the practical applications (like computation of the geoid) require knowledge of the Earth's gravity at the vicinity of the surface. Hence, processing of SGG data implicitly includes downward continuation, which is an unstable operation. Furthermore, the SGG data will be contaminated by colored (frequency-dependent) noise. The square root of noise power spectral density will be below 4 mE/$\sqrt{\text{Hz}}$ in the frequency range between 0.005 and 0.1 Hz, the so-called 'measurement band' (1 mE = 10^{-12} s^{-2}). Outside this interval (in particular, at higher frequencies) the noise may be significantly larger (Sünkel 2000; Alenia 2001). The consequence is that the SGG measurements are not sensitive to spherical harmonics of very high degrees/orders. According to our simulations, the maximum spherical harmonic degree resolvable from GOCE SGG data will be in the range 260–280. Nevertheless, it makes sense to set the maximum degree in the data processing beyond the resolution limits (e.g. to 300) in order to guarantee that the information content of the collected SGG data is fully preserved. Such a strategy suggests, however, that the spherical harmonic coefficients cannot be determined solely from the SGG data, so that some a priori information has to be added. A routine way to do this is to apply a regularization. Typically, the influence of the regularization grows with increasing spherical harmonic degree, so that the spherical harmonic coefficients (or, more precisely, coefficient corrections) related to the highest degrees gradually approach zero. If the truncation degree is sufficiently high, there is no longer a clear distinction between the commission error in the solution, which reflects the propagated noise, and the omission error, which is caused by the truncation of the spherical harmonic expansion.

In general a regularization may play a dual role. On the one hand, it is needed every time when an inverse problem under consideration is ill-posed, even if the input data are noise free. In this case, we must use a regularization in order to perform the inversion technically: otherwise, inversion software may crash. If the data are noise free, choosing a regularization parameter is not usually a problem because the inversion results are barely sensitive to this choice; it may even be enough to take the smallest regularization parameter that still guarantees stable working of the software. On the other hand, regularization may play the role of a low-pass filter that suppresses high-frequency errors in a model due to propagated data noise. If data are noisy, application of a regularization may be important even if a problem is, strictly speaking, not ill-posed (although an ill-posedness, naturally, magnifies noise). In this situation, choosing the optimal regularization parameter may be less trivial. In the context of SGG data processing, the primary goal of regularization is just to suppress model errors at the highest spatial frequencies.

A general concept of regularization was originally developed by Tikhonov (Tihonov 1963a, b; Tikhonov and Arsenin 1977). In particular, Tikhonov introduced a regularizing functional in the context of continuous inverse problems (Fredholm integral equations of the first kind). The regularizing functional minimizes the L_2-norm of the unknown function together with L_2-norms of its derivatives (in an a priori specified proportion). A regularization is called Tikhonov regularization of the order k if the highest order of the derivative included in the regularizing functional is k. Tikhonov has also developed a regularization concept in the context of discrete problems (in particular, inversion of ill-posed matrices).

The issue of regularization includes two aspects: (1) the optimal choice of the regularization technique (i.e. of the regularizing functional or the regularization matrix) and (2) the optimal choice of the regularization parameter. A routine regularization technique applied in a computation of spherical harmonic coefficients from satellite measurements makes use of the Kaula rule of thumb (Kaula 1966). According to this, elements of the regularization matrix are set equal to the fourth power of the current degree l. Kaula's rule of thumb prescribes also the regularization parameter to be used: 10^{10}. A number of alternative regularization techniques have been considered specifically in the context of satellite gravity gradiometry by Xu (1992), Ilk (1993), Bouman and Koop (1998), Bouman (2000), Lonkhuyzen et al. (2001), Koch and Kusche (2002), and Kusche and Mayer-Gürr (2002). Furthermore, we would like to mention in particular the studies of Kusche and Klees (2002a, b), who systematically compared diagonal regularization matrices, elements of which were proportional to different powers of the degree l. It was concluded that the quality of the model obtained is reasonably insensitive to the choice of the regularization matrix unless the matrix is specified as the unit one: in that case, the quality of the model deteriorates.

As far as the optimal choice of the regularization parameter is concerned, the papers of Koch and Kusche (2002) and Kusche and Klees (2002b) deserve special attention because various heuristic choice rules have been considered therein: the L-curve criterion and the generalized cross-validation in the former publication and the variance component estimation technique in the latter one. 'Heuristic rules' means in this context that these rules are independent of a priori knowledge of the noise level in the data. We expect that in practice we will be unable to rely upon this sort of information. First, pre-launch estimations of the hardware accuracy may differ from the real behavior in the orbit. Second, a functional model used for SGG data processing may suffer from an incompleteness, which will manifest itself as an extra noise in the data. Third, selection of the optimal regularization parameter on the basis of noise in the data is very sensitive to errors in the estimation of noise properties. For these reasons, heuristic rules seem to be preferable. Furthermore, a model obtained with an heuristic parameter choice rule offers an independent way to assess data noise: it is enough to simulate data on the basis of the obtained model and subtract them from the observations.

The scope of this paper is the regularization in the context of the GOCESOFT software, which is aimed at transformation of data to be acquired by the GOCE

satellite into parameters of the Earth's gravity field. This software exploits a fast and accurate algorithm for SGG data processing (Ditmar and Klees 2002; Ditmar et al. 2003), which is based on the pre-conditioned conjugate gradient (PCCG) method. According to the latest estimations, GOCESOFT is capable of processing the whole set of GOCE SGG data within only 1 hour. Thanks to this, we are able to consider different aspects of the regularization in a much more realistic environment than that of any other study made so far. The first goal of our study is to continue a systematic comparison of different regularization techniques (i.e. regularization matrices). Moreover, we clarify the physical meaning of different regularization matrices by relating them to certain smoothness properties of the gravitational potential. In other words, we establish a link between the discrete and the continuous Tikhonov regularization. In particular, we demonstrate that application of Kaula's rule of thumb can be considered in practice as a second-order Tikhonov regularization. The second goal of our research is to investigate an heuristic parameter choice rule in a realistic experimental setup; the generalized cross-validation technique has been selected for this purpose.

In our numerical study, we compare both the quality of the models obtained and the numerical performance of computations. One of the direct applications of this study is the assessment of the accuracy of an Earth gravity model that can be deduced from the whole set of GOCE SGG data.

2 Data processing methodology

In the paper presented, we limit ourselves to the static gravity field of the Earth. Let this field be represented by a series of spherical harmonics. Furthermore, suppose that the contribution of a reference gravity field is subtracted from the collected SGG data during the pre-processing (in practice, the reference field will be specified according to the best gravity field model available). The remaining signal in the SGG data can be used to determine parameters of the disturbing potential – the correction to be applied to the reference gravity field. Furthermore, we truncate the spherical harmonic expansion describing the disturbing potential, so that only orders and degrees not exceeding a certain maximum degree $L_{\max}$ are taken into consideration. On the one hand, such a truncation is needed in order to represent the unknown function by means of a limited set of unknown parameters. On the other hand, this truncation is fully justified in the case of SGG data because their resolution is limited, so that they cannot be used to determine coefficients related to very high degrees and orders anyway. Our simulations show that setting the maximum degree to 300 is sufficient to avoid a loss of information contained in the acquired SGG data.

The explicit expression for the disturbing potential $V(r,\theta,\lambda)$ can be written as follows:

$$V(r,\theta,\lambda) = \frac{GM}{R}\sum_{l=2}^{L_{\max}}\left(\frac{R}{r}\right)^{l+1} \times \sum_{m=0}^{l}\left\{C_{lm}Y_{lm}^{(C)}(\theta,\lambda) + S_{lm}Y_{lm}^{(S)}(\theta,\lambda)\right\} \quad (1)$$

where r,θ,λ are the spherical coordinates; G is the universal gravitational constant; M is the Earth's mass; R is the semi-major axis of a reference ellipsoid; C_{lm} and S_{lm} are the spherical harmonic coefficients representing the disturbing potential; $Y_{lm}^{(C)}(\theta,\lambda)$ and $Y_{lm}^{(S)}(\theta,\lambda)$ are the 4π-normalized surface spherical harmonics

$$\begin{aligned} Y_{lm}^{(C)}(\theta,\lambda) &= \bar{P}_{lm}(\cos\theta)\cos(m\lambda) \\ Y_{lm}^{(S)}(\theta,\lambda) &= \bar{P}_{lm}(\cos\theta)\sin(m\lambda) \end{aligned} \quad (2)$$

with $\bar{P}_{lm}(\cos\theta)$ the normalized associated Legendre functions.

The disturbing potential depends linearly on the spherical harmonic coefficients. Therefore, the pre-processed SGG measurements – second derivatives of the disturbing potential – can also be linearly related to them. Furthermore, the measurements will be contaminated by noise. Then, the following vector equation holds:

$$\mathbf{d} = \mathbf{A}\mathbf{x} + \boldsymbol{\eta} \quad (3)$$

where $\mathbf{d}$ is the data vector, $\mathbf{x}$ is the model vector comprised of the spherical harmonic coefficients, $\boldsymbol{\eta}$ is the vector of data errors, and $\mathbf{A}$ is the design matrix. An explicit representation of the design matrix $\mathbf{A}$ is discussed, in particular, in Ditmar and Klees (2002).

Assuming that noise in the data is random and Gaussian, we can represent the functional model of observations as a standard Gauss–Markov model

$$E\{\mathbf{d}\} = \mathbf{A}\mathbf{x}, \quad D\{\mathbf{d}\} = D\{\boldsymbol{\eta}\} = \mathbf{C_d} \quad (4)$$

where E and D denote the expectation and dispersion operators, respectively, and $\mathbf{C_d}$ is the noise covariance matrix. Then, a reasonable estimation $\hat{\mathbf{x}}$ of the Earth's gravity field can be obtained by a minimization of the quadratic objective function

$$\tilde{\boldsymbol{\Phi}}(\hat{\mathbf{x}}) = (\mathbf{A}\hat{\mathbf{x}} - \mathbf{d})^T\mathbf{C_d}^{-1}(\mathbf{A}\hat{\mathbf{x}} - \mathbf{d}) + \alpha\hat{\mathbf{x}}^T\mathbf{R}\hat{\mathbf{x}} \quad (5)$$

where $\mathbf{R}$ is a regularization matrix and α is a (non-negative) regularization parameter. The first term in the objective function of Eq. (5) forces the model to fit the data, whereas the second term represents the regularization.

The objective function of Eq. (5) is equal (up to a constant) to the following one:

$$\boldsymbol{\Phi}(\hat{\mathbf{x}}) = \hat{\mathbf{x}}^T\left(\mathbf{A}^T\mathbf{C_d}^{-1}\mathbf{A} + \alpha\mathbf{R}\right)\hat{\mathbf{x}} - 2\hat{\mathbf{x}}^T\mathbf{A}^T\mathbf{C_d}^{-1}\mathbf{d} \quad (6)$$

In order to minimize this objective function, the GOCESOFT software exploits the PCCG method (Hestenes and Stiefel 1952; Bertsekas 1982). The PCCG method works iteratively. The basic operation at each iteration is the application of the normal matrix

$$\mathbf{N} = \mathbf{A}^T \mathbf{C}_\mathbf{d}^{-1} \mathbf{A} + \alpha \mathbf{R} \tag{7}$$

to a certain vector **p**. Importantly, this operation does not require that the normal matrix is known explicitly. Instead, we can carry out a sequence of matrix–vector multiplications as follows:

$$\mathbf{Np} = \mathbf{A}^T \left(\mathbf{C}_\mathbf{d}^{-1} (\mathbf{Ap}) \right) + \alpha \mathbf{Rp} \tag{8}$$

The operation **Ap** is the spherical harmonic synthesis. The multiplication of the matrix $\mathbf{C}_\mathbf{d}^{-1}$ to the resulting vector can be interpreted as filtering (Schuh 1996; Klees et al. 2003). Applying the matrix $\mathbf{A}^\mathbf{T}$ to the vector obtained after filtering is called the (spherical harmonic) co-synthesis. Thanks to recently developed algorithms for fast synthesis and co-synthesis (Ditmar et al. 2003), these two operations can be performed extremely efficiently. Finally, the operation $\alpha\mathbf{Rp}$ is the regularization. The number of PCCG iterations depends on the choice of the pre-conditioner. In our case, a block-diagonal approximation of the normal matrix (Colombo 1986; Ditmar and Klees 2002) is used for this purpose; such a choice reduces the number of iterations to only a few. The main scope of this paper is regularization.

3 Choice of the regularization matrix

3.1 Zero-order Tikhonov (ZOT) regularization

In many inverse problems, the regularization matrix is just set equal to the unit one. In our case, this is equivalent to minimizing the L_2-norm of the disturbing potential near the Earth's surface [or, more precisely, at the sphere of radius R, where R is defined in the same way as in the expression for the disturbing potential of Eq. (1)]. Let us show this. Assume that the regularization term in the objective function of Eq. (5) is defined as

$$\Phi_R^{(\mathrm{ZOT})}(\hat{\mathbf{x}}) = \int\limits_{\Omega_R} V^2(r, \theta, \lambda) \, \mathrm{d}\Omega_R \tag{9}$$

where Ω_R denotes the sphere of radius R.

The surface spherical harmonics form a set of orthogonal functions. Hence substitution of the expression for the disturbing potential of Eq. (1) into the regularization condition of Eq. (9) and changing the order of integration and summations yields

$$\Phi_R^{(\mathrm{ZOT})}(\hat{\mathbf{x}}) = 4\pi (GM)^2 \sum_{l=2}^{L_{\max}} \sum_{m=0}^{l} \left(C_{lm}^2 + S_{lm}^2 \right) \tag{10}$$

or in matrix form

$$\Phi_R^{(\mathrm{ZOT})}(\hat{\mathbf{x}}) = 4\pi (GM)^2 \hat{\mathbf{x}}^T \mathbf{R}^{(\mathbf{ZOT})} \hat{\mathbf{x}} \tag{11}$$

where matrix $\mathbf{R}^{(\mathbf{ZOT})}$ is unit.

The constant factor $4\pi(GM)^2$ in Eq. (11) can be ignored because the regularization matrix has to be scaled anyway by applying a regularization parameter. Thus, the regularization exploiting the unit regularization matrix can indeed be considered as a zero-order Tikhonov (ZOT) regularization.

3.1.1 First-order Tikhonov (FOT) regularization

By analogy to the ZOT regularization, the first-order Tikhonov (FOT) regularization can be introduced. In this case, first-order derivatives of the disturbing potential should be minimized, rather than the disturbing potential itself. More specifically, let us understand the FOT regularization as minimization of the horizontal gradient of the gravitational potential near the Earth's surface

$$\Phi_R^{(\mathrm{FOT})}(\hat{\mathbf{x}}) = \int\limits_{\Omega_R} \left(\nabla_H V(r, \theta, \lambda) \right)^2 \mathrm{d}\Omega_R \tag{12}$$

where ∇_H is the surface gradient operator

$$\nabla_H = \begin{pmatrix} 0 \\ \frac{1}{r} \frac{\partial}{\partial \theta} \\ \frac{1}{r \sin\theta} \frac{\partial}{\partial \lambda} \end{pmatrix}$$

According to Green's formulas on a sphere (Meissl 1971, p. 12), Eq. (12) can be represented as

$$\Phi_R^{(\mathrm{FOT})}(\hat{\mathbf{x}}) = -\int\limits_{\Omega_R} V(r, \theta, \lambda) \Delta_H V(r, \theta, \lambda) \, \mathrm{d}\Omega_R \tag{13}$$

where Δ_H is the Laplace–Beltrami operator or surface Laplacian

$$\Delta_H = \frac{1}{r^2 \sin\theta} \frac{\partial}{\partial \theta} \left(\sin\theta \frac{\partial}{\partial \theta} \right) + \frac{1}{r^2 \sin^2\theta} \frac{\partial^2}{\partial \lambda^2}$$

By definition, the gravitational potential represented by spherical harmonics is a harmonic function

$$\Delta V(r, \theta, \lambda) = \frac{1}{r^2} \frac{\partial}{\partial r} \left(r^2 \frac{\partial}{\partial r} \right) V(r, \theta, \lambda) + \Delta_H V(r, \theta, \lambda) = 0$$

Therefore, it holds that

$$\begin{aligned} \Delta_H V(r, \theta, \lambda) \Big|_{r=R} &= -\frac{1}{r^2} \frac{\partial}{\partial r} \left(r^2 \frac{\partial}{\partial r} \right) V(r, \theta, \lambda) \Big|_{r=R} \\ &= -\frac{GM}{R^3} \sum_{l=2}^{L_{\max}} l(l+1) \\ &\quad \times \sum_{m=0}^{l} \left\{ C_{lm} Y_{lm}^{(C)}(\theta, \lambda) + S_{lm} Y_{lm}^{(S)}(\theta, \lambda) \right\} \end{aligned} \tag{14}$$

After substituting Eqs. (1) and (14) into the functional of Eq. (13) and taking the orthogonality properties into account, we have

$$\Phi_R^{(\mathrm{FOT})}(\hat{\mathbf{x}}) = 4\pi \left[\frac{GM}{R} \right]^2 \hat{\mathbf{x}}^T \mathbf{R}^{(\mathbf{FOT})} \hat{\mathbf{x}} \tag{15}$$

where the matrix $\mathbf{R}^{(\mathbf{FOT})}$ is defined as

$$\left\{\mathbf{R}^{(\mathrm{FOT})}\right\}_{ij} = \delta_{ij} l(i)(l(i)+1) \tag{16}$$

with $l(i)$ being the degree related to the row (or column) number i. Thus, the FOT regularization can be implemented as easily as the ZOT regularization.

3.1.2 Second-order Tikhonov (SOT) regularization and Kaula regularization

By analogy to the ZOT and the FOT regularization, we can also introduce the second-order Tikhonov (SOT) regularization. Let us understand the SOT regularization as minimization of the surface Laplacian of the gravitational potential near the Earth's surface

$$\Phi_R^{(\mathrm{SOT})}(\hat{\mathbf{x}}) = \int_{\Omega_R} \left(\Delta_H V(r,\theta,\lambda)\right)^2 \mathrm{d}\Omega_R \tag{17}$$

Again we can use Eq. (14), which yields, in combination with the orthogonality of surface spherical harmonics

$$\Phi_R^{(\mathrm{SOT})}(\hat{\mathbf{x}}) = 4\pi\left[\frac{GM}{R^2}\right]^2 \sum_{l=L_{\min}}^{L_{\max}} l^2(l+1)^2 \sum_{m=0}^{l}\left(C_{lm}^2 + S_{lm}^2\right) \tag{18}$$

or in matrix form

$$\Phi_R^{(\mathrm{SOT})}(\hat{\mathbf{x}}) = 4\pi\left[\frac{GM}{R^2}\right]^2 \hat{\mathbf{x}}^T \mathbf{R}^{(\mathbf{SOT})} \hat{\mathbf{x}} \tag{19}$$

where the matrix $\mathbf{R}^{(\mathbf{SOT})}$ is defined as

$$\left\{\mathbf{R}^{(\mathbf{SOT})}\right\}_{ij} = \delta_{ij} l^2(i)(l(i)+1)^2 \tag{20}$$

Elements of the SOT regularization matrix of Eq. (20) related to large degrees l are very close to those in the Kaula regularization matrix $\mathbf{R}^{(\mathbf{K})}$ which is based on the Kaula rule of thumb

$$\left\{\mathbf{R}^{(\mathbf{K})}\right\}_{ij} = \delta_{ij} l^4(i) \tag{21}$$

On the other hand, elements related to small degrees typically play no role because, when multiplied with a proper regularization parameter, they are orders of magnitude smaller than the elements of the unregularized normal matrix $\mathbf{A}^T\mathbf{C}_{\mathbf{d}}^{-1}\mathbf{A}$. Thus, the behavior of the SOT regularization is practically identical to that of the Kaula regularization.

4 Finding the optimal regularization parameter

The accuracy of an inversion procedure may be strongly dependent on the choice of the regularization parameter. The parameter choice rule implemented in the GOCESOFT software is based on the generalized cross-validation (GCV) method because previous studies (Kusche and Klees 2002b) have demonstrated its good performance. We have slightly modified an implementation of the GCV presented by Kusche and Klees (2002b) in order to improve the numerical efficiency.

The philosophy of the GCV method is based on the leave-out-one or 'jackknife' idea, which has been well known in geodetic testing theory for a very long time. Assume that a certain observation in the collected data set is omitted and the corresponding solution is found. The same can be repeated with all the observation points in succession. Then, a regularization parameter α is considered as the optimal one if it gives, on average, best predictions of missing observations.

It can be shown (Golub and Wahba 1979; Wahba 1990; Kusche and Klees 2002b) that in practice this idea can be implemented as just a 1-D minimization of the so-called GCV function

$$f^{\mathrm{gcv}}(\alpha) = \frac{n(\mathbf{A}\mathbf{x}_\alpha - \mathbf{d})^T\mathbf{C}_{\mathbf{d}}^{-1}(\mathbf{A}\mathbf{x}_\alpha - \mathbf{d})}{(n - \mathcal{T}_\alpha)^2} \tag{22}$$

where n is the number of unknowns; $\mathbf{x}_\alpha$ is the solution obtained with a given regularization parameter α; $\mathcal{T}_\alpha = \mathrm{trace}(\mathbf{Q}^\alpha)$; and $\mathbf{Q}^\alpha$ is the influence matrix

$$\mathbf{Q}^\alpha = \mathbf{A}(\mathbf{A}^T\mathbf{C}_{\mathbf{d}}^{-1}\mathbf{A} + \alpha\mathbf{R})^{-1}\mathbf{A}^T\mathbf{C}_{\mathbf{d}}^{-1} \tag{23}$$

In large-scale problems, like satellite gravity gradiometry, an explicit computation of the influence matrix and, therefore, of its trace is very time consuming. One way out is to use stochastic trace estimators (Girard 1989). Let us introduce a random vector $\mathbf{z}$ of length n with $E\{\mathbf{z}\} = 0$ and $D\{\mathbf{z}\} = \mathbf{I}$. Then, an unbiased trace estimation can be obtained with the expression

$$\hat{\mathcal{T}_\alpha} = \mathbf{z}^T\mathbf{Q}^\alpha\mathbf{z} \tag{24}$$

This expression may be better understood if the matrix–vector multiplication is written in the component-wise form with diagonal and off-diagonal terms being grouped separately

$$\begin{aligned}\mathbf{z}^T\mathbf{Q}^\alpha\mathbf{z} &= \sum_{i,j=1}^{n}\{\mathbf{Q}^\alpha\}_{ij}\{\mathbf{z}\}_i\{\mathbf{z}\}_j \\ &= \sum_{i=1}^{n}\{\mathbf{Q}^\alpha\}_{ii}\{\mathbf{z}\}_i^2 + \sum_{\substack{i,j=1\\ i\neq j}}^{n}\{\mathbf{Q}^\alpha\}_{ij}\{\mathbf{z}\}_i\{\mathbf{z}\}_j\end{aligned} \tag{25}$$

After applying the expectation operator, off-diagonal terms in Eq. (25) vanish, so that we have

$$\begin{aligned}E\left[\mathbf{z}^T\mathbf{Q}^\alpha\mathbf{z}\right] &= \sum_{i=1}^{n}\{\mathbf{Q}^\alpha\}_{ii}E\left[\{\mathbf{z}\}_i^2\right] \\ &= \sum_{i=1}^{n}\{\mathbf{Q}^\alpha\}_{ii} = \mathrm{trace}(\mathbf{Q}^\alpha)\end{aligned} \tag{26}$$

Application of the expectation operator implies that a number of random vectors $\mathbf{z}$ are used with the subsequent averaging of trace estimations. However, for large-scale problems like the processing of GOCE SGG data it is sufficient to consider only one random vector (Golub and Matt 1997; Kusche and Klees 2002b).

Thus, the trace of the influence matrix can be estimated as

$$\hat{\mathcal{T}}_\alpha = \mathbf{z}^T\mathbf{A}(\mathbf{A}^T\mathbf{C}_\mathbf{d}^{-1}\mathbf{A} + \alpha\mathbf{R})^{-1}\mathbf{A}^T\mathbf{C}_\mathbf{d}^{-1}\mathbf{z} \tag{27}$$

In practice, the computation of $\hat{\mathcal{T}}_\alpha$ starts from the initialization phase when (1) a random vector $\mathbf{z}$ is generated and (2) auxiliary vectors $\mathbf{y_1} = \mathbf{A}^T\mathbf{C}_\mathbf{d}^{-1}\mathbf{z}$ and $\mathbf{y_2} = \mathbf{A}^T\mathbf{z}$ are computed. After that, for each considered regularization parameter α: (1) the system of linear equations $(\mathbf{A}^T\mathbf{C}_\mathbf{d}^{-1}\mathbf{A} + \alpha\mathbf{R})\mathbf{q}_\alpha = \mathbf{y_1}$ is solved and (2) the trace estimator is computed as $\hat{\mathcal{T}}_\alpha = \mathbf{y_2}^T\mathbf{q}_\alpha$.

In this way, each computation of the GCV function of Eq. (22) requires only two inversion runs: one for the numerator (to obtain the model vector $\mathbf{x}_\alpha$) and one for the denominator. In order to find the minimum of the GCV function, one of the methods for 1-D numerical minimization can be applied.

5 Numerical experiments

5.1 Data sets

Two sets of noisy SGG data have been simulated for the purpose of a numerical study. They are referred to as the 'short' and the 'long' data set.

5.1.1 Short data set

1. Orbit: realistic 2-month repeat GOCE orbit, 961 revolutions, mean inclination 96.77°, radius 6647 ± 12 km (average elevation above the equator is about 268 km).
2. Observations: diagonal components of the gravity gradients tensor (i.e. components *XX*, *YY*, and *ZZ*); 5-s sampling rate (1 036 801 observation points).
3. 'True' disturbing potential: difference between the OSU91A model (Rapp et al.1991) truncated at degree/order 300 and the GRS80 normal field (Moritz 1980).
4. (Square root of) the noise power spectral density (PSD): same for all three components, and defined by means of the analytic function

$$\sigma(f) = \frac{\sigma_0}{1 - \mathrm{e}^{-\frac{f}{f_0}}} \tag{28}$$

where $\sigma_0 = 3.2\,\mathrm{mE}/\sqrt{\mathrm{Hz}}$ and $f_0 = 27\,\mathrm{cpr}/T_r \approx 0.005$ Hz, where 'cpr' stands for cycles per revolution, and T_r is the average revolution period ($\approx$5400 s). A plot of this analytic function is shown in Fig. 1a. In this case, elements of the matrix $\mathbf{C}_\mathbf{d}^{-1}$ can also be computed analytically (Ditmar and Klees 2002).

The issue of building the Earth's gravity field model from such a data set may be raised when temporal gravitational variations have to be detected, so that the whole set of acquired data is split into relatively short subsets, each of which is treated separately.

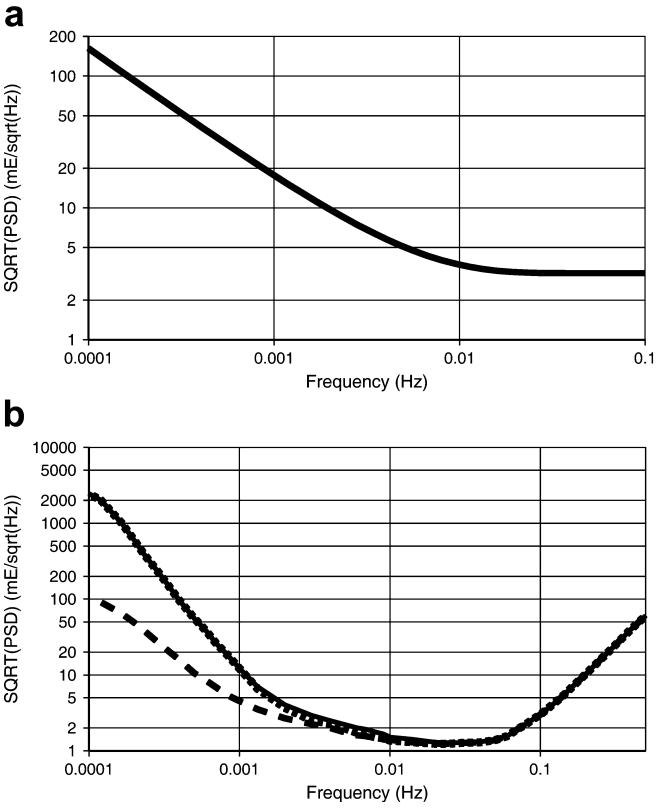

Fig. 1. Square root of the noise PSD used in the simulation of **a** the short and the long **b** data sets. *Dotted*, *dashed*, and *solid lines* in the bottom picture correspond to the *XX*-, *YY*-, and *ZZ*-components of the gravity gradients tensor, respectively

5.1.2 Long data set

1. Orbit: realistic 6-month non-repeat GOCE orbit, 2903.16 revolutions, mean inclination 96.65°, radius 6640 ± 12 km (the average elevation above the equator is about 262 km).
2. Observations: diagonal components of the gravity gradients tensor; 1-s sampling rate (15 638 401 observation points).
3. 'True' disturbing potential: same as for the short data set.
4. (Square root of) the noise PSD: a digital version of a realistic noise behavior (Sünkel 2000), (see Fig. 1b). Notice that the noise PSD is not the same for different components. Application of the matrix $\mathbf{C}_\mathbf{d}^{-1}$ to a vector is implemented as two sequential operations of ARMA filtering ('ARMA' means auto-regressive moving-average). Algorithms for deriving optimal ARMA-filter coefficients from a noise PSD are discussed by Klees and Broersen (2002) and Klees et al. (2003).

The long data set basically imitates the SGG data that will be acquired by the GOCE satellite during one of the two half-year observation periods. Such (or even longer) data sets will be handled in computing a model of the static Earth's gravity field.

The minimum and maximum degree solved for are always set equal to 2 and 300, respectively. All numerical

experiments have been carried out on the SGI Origin 3800 computer.

5.2 Comparison of regularization matrices

The first goal of our numerical study is to compare three of the regularization techniques presented above: ZOT, FOT, and Kaula. The SOT regularization is not considered because, as we have pointed out, it is practically equivalent to the Kaula regularization. The quality of a model obtained is quantified as the RMS deviation from the true one in terms of geoid heights and, occasionally, in terms of gravity anomalies. The quantities are computed in the latitudinal band $\pm 80^\circ$ with step 0.5° in both the latitudinal and the longitudinal direction. The polar areas are eliminated from the evaluation because they are not covered by measurements. We find this evaluation procedure more appropriate than the traditional ones where there is no distinction between polar and non-polar areas. It may be claimed that our precaution is not important because the polar areas occupy only a few percent of the Earth's surface. However, the absence of SGG measurements in these areas makes the corresponding model errors orders of magnitude larger than the errors in areas covered by data. Therefore, errors in polar areas may have a significant influence, thus making an evaluation less fair.

Unfortunately, the straightforward implementation of both the ZOT and the FOT regularization may not provide a meaningful solution. Typical results of the data processing (obtained from the short data set) are shown in Fig. 2. This behavior can be explained by a low magnitude of the normal matrix elements related to the lowest degrees (Fig. 3). This is a direct consequence of the filtering we apply in order to down-weight the contribution of frequencies where the noise level is high. Due to the filtering, the low-frequency content in both the data and the columns of the design matrix is suppressed. Furthermore, the entire content of the columns related to the low-order coefficients is of a low frequency [roughly speaking, a column related to degree l contains only frequencies up to 'l' cycles per revolution (Koop 1993; Ditmar and Klees 2002)]. As a result, elements of the regularization matrix may become comparable with those of the unregularized normal matrix or, in the case of the ZOT regularization, even dominant (Fig. 3). For this reason, the low-order coefficients describing the disturbing potential become close to zero. Therefore, the model obtained is close to the reference one, i.e. wrong. A possible magnitude of the model errors can be seen in Fig. 2a, which shows, in essence, just the difference between low-frequency contents in the true and the reference models.

In order to cope with this unpleasant effect, we have modified the regularization matrices so that the coefficients of the normal matrix related to small degrees are excluded from the regularization. In other words, the expressions for the ZOT and FOT regularization matrices now read

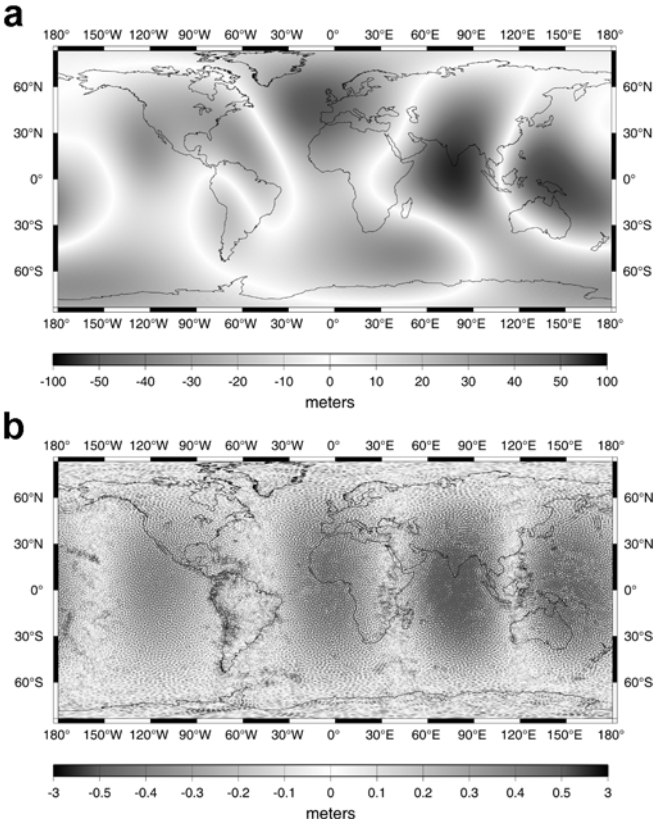

Fig. 2. Processing of the short data set with **a** the ZOT and **b** the FOT regularization; maps of geoid height errors. The regularization parameters are 300×10^{17} (ZOT) and 500×10^{12} (FOT). All degrees in the normal matrix are subject to the regularization. The RMS geoid height error is equal to 26.8 m (ZOT) and 35.4 cm (FOT)

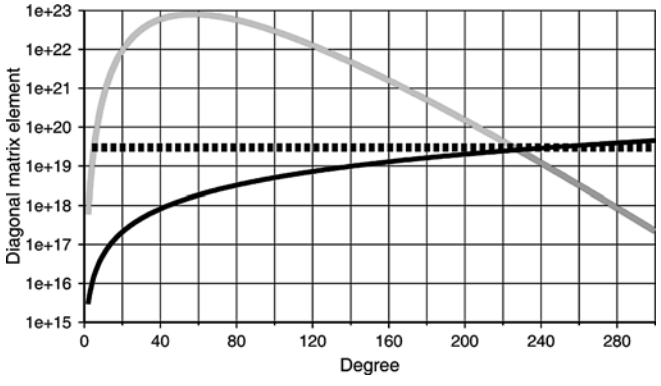

Fig. 3. Processing of the short data set. *Black lines* show dependence of elements in the regularization matrices (scaled by corresponding regularization parameters) on the current degree l; *dotted* and *solid lines* correspond to the ZOT and FOT regularization, respectively. *Grey line* shows the dependence of the diagonal elements in the unregularized normal matrix on the current degree l; the elements are averaged over orders m. A block-diagonal approximation of the normal matrix has been used to produce this plot

$$\left\{\mathbf{R}^{(\mathbf{ZOT})}\right\}_{ij} = \begin{cases} 0 & \text{if } l \le L_{\text{thr}} \\ \delta_{ij} & \text{otherwise} \end{cases} \tag{29}$$

and

$$\left\{\mathbf{R}^{(\mathbf{FOT})}\right\}_{ij} = \begin{cases} 0 & \text{if } l \le L_{\text{thr}} \\ \delta_{ij} l(i)(l(i)+1) & \text{otherwise} \end{cases} \tag{30}$$

In practice, the threshold degree L_{thr} is set equal to 30, which corresponds, in view of the discussion above, to the frequency 6×10^{-3} Hz. As can be seen from Fig. 1, this frequency approximately coincides with the upper bound of the range that contains strong low-frequency noise. Hence, the modified regularization influences only the elements that are not significantly suppressed by filtering.

The idea of the updated regularization can be also interpreted as splitting the vector of unknowns into the low-frequency and the high-frequency parts: $\mathbf{x} = \mathbf{x}^{\mathbf{lf}} + \mathbf{x}^{\mathbf{hf}}$, where $\mathbf{x}^{\mathbf{lf}}$ contains degrees from 2 to L_{thr} and $\mathbf{x}^{\mathbf{hf}}$ degrees from $L_{\text{thr}} + 1$ to $L_{\max}$. Then, the regularization condition of Eq. (9) or (12) is supposed to be applied only to the high-frequency part of the disturbing potential.

Processing of the short data set with the updated FOT regularization (all other parameters being as before) leads to the model presented in Fig. 4a. Obviously, the target is achieved: the bias at low degrees is eliminated. The result obtained with the updated ZOT regularization is not shown because it is very similar to that presented in Fig. 4a. Furthermore, processing of the long data set with the updated FOT regularization also demonstrates an ability to recover the low-frequency content of the model properly (Fig. 4b).

Importantly, selection of the threshold degree L_{thr} in the range where elements of the normal matrix dominate over those in a regularization matrix guarantees that the model obtained is insensitive to L_{thr}. In order to check this, we have repeated the computations with the short data set, having specified L_{thr} equal to 26 and 41. The RMS geoid height difference with respect to the model shown in Fig. 4a (FOT regularization) turned out to be less than 0.4 mm. In the case of the ZOT regularization, the difference is larger but also tolerable: of the order of 3 mm.

From Fig. 4 we can also conclude that the remaining misfits between the true and calculated models are due to two reasons. The first reason is the propagated data noise, which is responsible for the 'orange-skin effect' – a homogeneous high-frequency pattern in the geoid error plot. The second reason is the high-frequency spatial variations of the Earth's gravity field in certain areas like mountains and subduction zones. These variations cannot be restored due to a smoothing effect of the regularization. By changing the regularization parameter, we can emphasize one or the other effect. Smaller regularization parameters cause stronger high-frequency noise in the solution (Fig. 5a), whereas larger regularization parameters lead to an excessive smoothness (Fig. 5b).

The dependence of the model accuracy on the regularization parameter for the ZOT, FOT, and Kaula

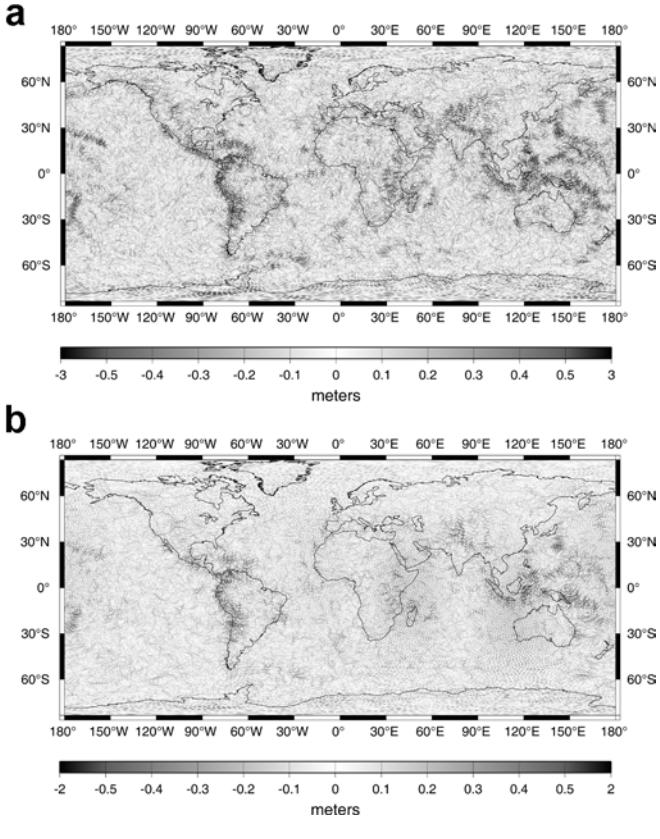

Fig. 4. Processing of **a** the short and **b** the long data set with the FOT regularization; maps of geoid height errors. Only degrees above 30 in the normal matrix are subject to the regularization. The regularization parameters are 500×10^{12} (short data set) and 1000×10^{12} (long data set). The RMS geoid height error is equal to 22.1 (short data set) and 14.9 cm (long data set)

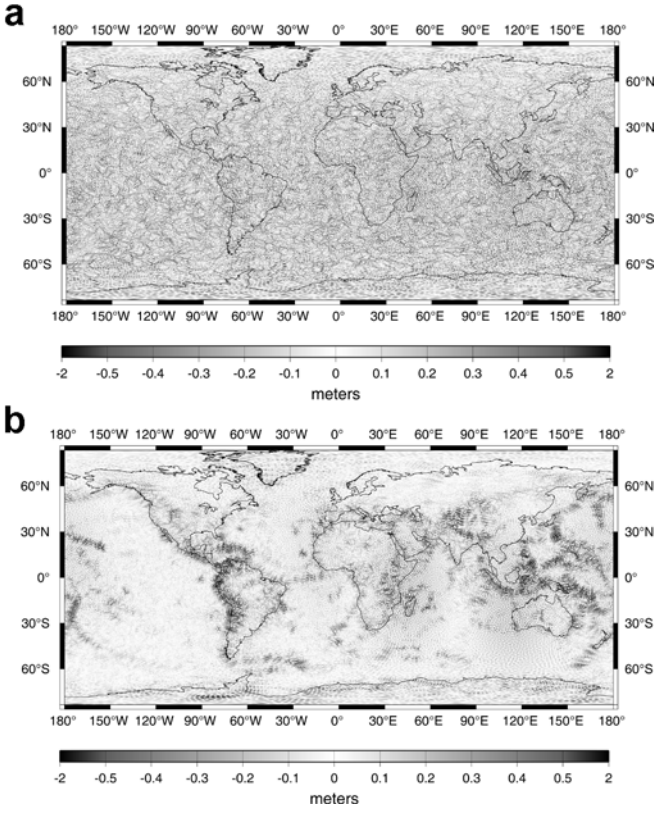

Fig. 5. Processing of the long data set with the FOT regularization; maps of geoid height errors. **a** The regularization parameter is too small (150×10^{12}). **b** The regularization parameter is too large ($15\,000 \times 10^{12}$). The RMS geoid height error is equal to 21.8 and 18.5 cm, respectively

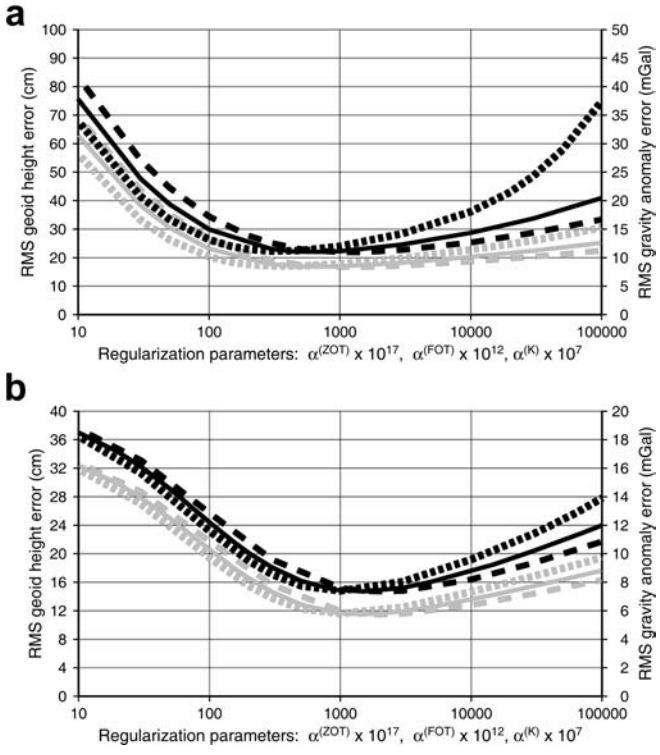

Fig. 6. Processing of **a** the short and **b** the long data set; dependence of the model accuracy on the regularization parameter. *Black* denotes the geoid height errors, *grey* the gravity anomaly errors. *Dotted*, *solid*, and *dashed curves* correspond to the ZOT, FOT, and Kaula regularization, respectively

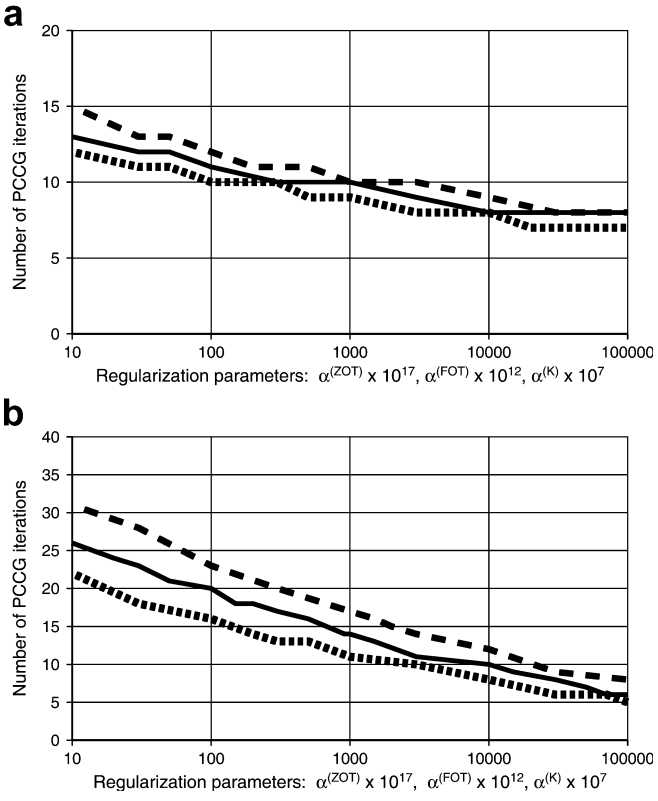

Fig. 7. Processing of **a** the short and **b** the long data set; dependence of the number of PCCG iterations on the regularization parameter. *Dotted*, *solid*, and *dashed curves* correspond to the ZOT, FOT, and Kaula regularization, respectively

regularizations is demonstrated, in terms of geoid heights and model anomalies, in Fig. 6. These plots show that the results presented in Fig. 4 are close to the optimum; this corresponds to such a selection of the regularization parameter that the two above-mentioned reasons for the misfits are in balance. Importantly, all the curves show a very similar behavior. An exception is the interval of relatively large regularization parameters, where the RMS geoid height error grows faster if the ZOT regularization is used (especially in the case of the short data set). In other words, the ZOT regularization demonstrates a larger sensitivity of the geoid configuration to the right choice of the regularization parameter than the other regularization techniques. This can be explained by the relatively large magnitude of the ZOT regularization matrix elements in the range of intermediate degrees l (cf. Fig. 3). By specifying an excessive regularization parameter, we can easily reach the situation where elements in the regularization and in the normal matrix become comparable.

Another important aspect is the numerical load related to different regularization matrices. Naturally, regularization itself is in all cases a very fast operation. However, various regularization techniques may change the condition number of the normal matrix in a different way, which can influence the number of required PCCG iterations. In order to shed light on this issue, we have plotted the number of PCCG iterations as a function of the regularization parameter for all three regularization techniques (Fig. 7). Importantly, the same stopping criterion has been applied in all examples: the difference between the geoid heights at two subsequent iterations has to be less than 0.1 mm on average and 1 mm at maximum (excluding the polar areas). It can be seen that there is only a minor dependence of the number of iterations on the regularization technique: Kaula regularization may require 20% more iterations than the FOT regularization, whereas the ZOT regularization may require 20% less iterations than the FOT regularization. It should be mentioned that the GOCESOFT software performs one iteration in about half a minute (provided that eight CPUs are used in the case of the short data set and 32 CPUs in the case of the long data set). Thus, each run takes in all cases not more than a few minutes.

Naturally, we can try alternative regularization techniques to those we have considered so far. In particular, Kusche and Klees (2002b) considered also diagonal regularization matrices, the elements of which were basically proportional to l^6 and l^8, where l is the degree related to the current row/column. Furthermore, Kusche and Klees (2002a) investigated a family of diagonal regularization matrices with elements varying continuously from $l^{2.8}$ to $l^{8.4}$. The conclusion drawn by Kusche and Klees (2002a) is that the quality of the model obtained is almost independent of the regularization matrix within these limits, the regularization

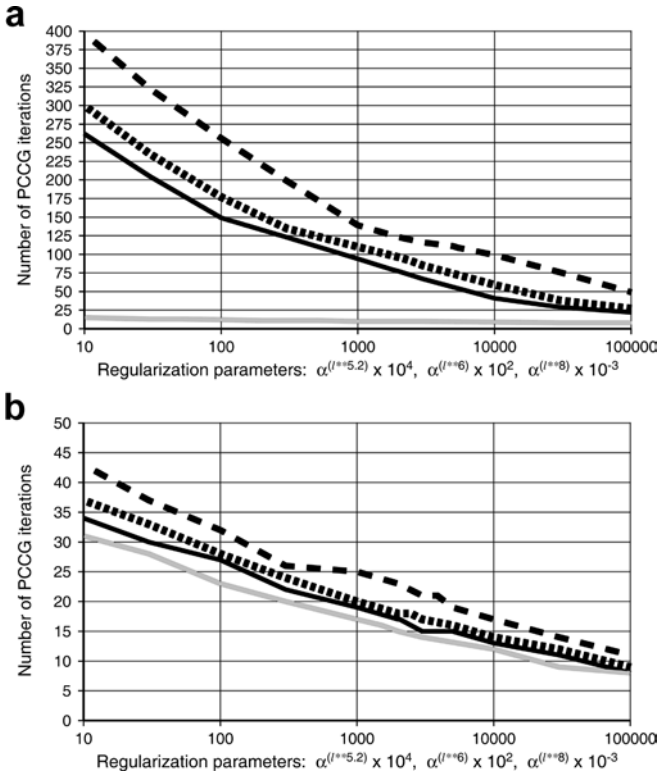

Fig. 8. Processing of **a** the short and **b** the long data set using other regularization techniques; dependence of the number of PCCG iterations on the regularization parameter. *Dotted*, *solid*, and *dashed black curves* correspond to diagonal regularization matrices with elements proportional to $l^{5.2}$, l^6, and l^8, respectively. As a reference, the curves related to the Kaula regularization (taken over from Fig. 7) are shown as *grey lines*

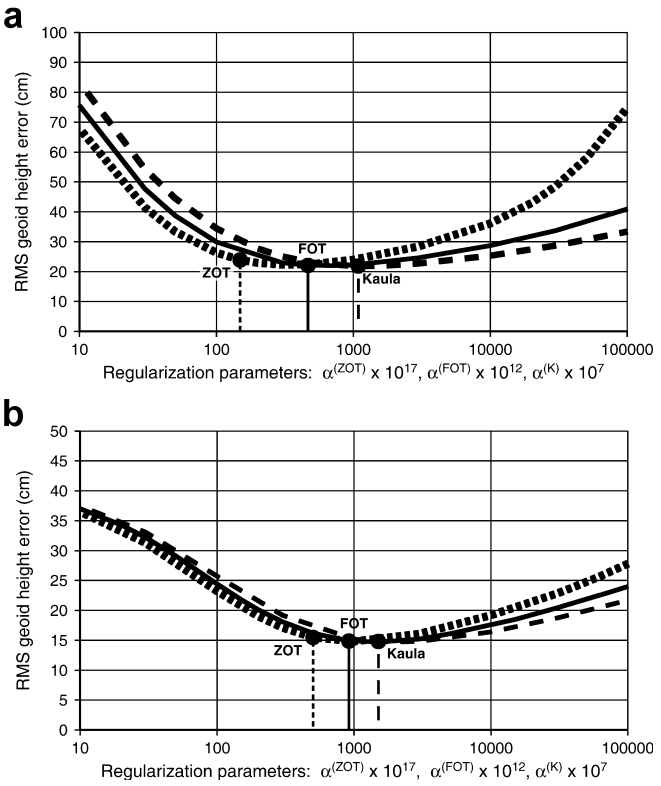

Fig. 9. Processing of **a** the short and **b** the long data sets. *Vertical lines* depict the regularization parameters found with the GCV method; *black circles* denote the corresponding RMS geoid height errors. *Dotted*, *solid*, and *dashed curves* show, as a reference, the dependence of the RMS geoid height error on the regularization parameter for ZOT, FOT, and Kaula regularization, respectively

matrix with elements proportional to $l^{5.2}$ being slightly superior to others. In order to verify these results, we have considered three more diagonal regularization matrices:

1. With elements proportional to $l^{5.2}$.
2. With elements proportional to l^6.
3. With elements proportional to l^8.

It turns out that the dependence of the geoid height errors on the regularization parameter in all three cases is very similar to that observed with the Kaula regularization (provided that the regularization parameters are properly re-scaled). In particular, improvement of the RMS geoid height error related to the best solution is negligible, if any: 21.8 vs 21.9 cm in case of the short data set and 14.6–14.7 vs 14.7 cm in case of the long data set. On the other hand, the required number of PCCG iterations has increased (Fig. 8). This is especially noticeable for the short data set, which is characterized by a relatively sparse spatial distribution of observation points. We explain such a behavior by an increased ill-posedness of the problem, which is caused by a too imbalanced application of the regularization over different degrees. For example, application of a proper regularization to the largest degrees leaves intermediate degrees, in essence, without any regularization. Thus, a regularization matrix with elements growing faster than Kaula's rule prescribes is probably not the best choice.

5.3 Heuristic selection of the regularization parameter

In the second part of our numerical study, we have tested the heuristic parameter choice rule based on the GCV method; both the short and the long data sets are considered. The results obtained are presented in Fig. 9, which shows the regularization parameters selected by the GCV method. It can be seen that in all the considered cases the GCV method offers a regularization parameter that is very close to the optimal one, although it may be slightly underestimated. This conclusion is further supported by the results shown in Table 1. The deviation of the best solution from the GCV-based one is especially noticeable in the case of the ZOT regularization. This can be explained by an increased sensitivity of a ZOT solution to the right choice of the regularization parameter.

At first glance, an underestimation of the regularization parameter is a drawback of the GCV method. The RMS geoid height error is, however, only one of the possible criteria for assessing the quality of the solution. An alternative is to analyze the maximum geoid height error, and from this point of view much smaller

Table 1. Comparison of the gravity field models obtained with the best regularization parameters (in the sense of the RMS geoid height error) with those found after applying the GCV method

	Minimum RMS choice		GCV choice	
	Regularization parameter	RMS geoid error (cm)	Regularization parameter	RMS geoid error (cm)
Short data set				
ZOT	300×10^{17}	22.3	149×10^{17}	23.9
FOT	700×10^{12}	22.0	465×10^{12}	22.1
Kaula	1200×10^{7}	21.9	1089×10^{7}	21.9
Long data set				
ZOT	1000×10^{17}	14.8	503×10^{17}	15.5
FOT	1500×10^{12}	14.7	916×10^{12}	14.9
Kaula	2000×10^{7}	14.7	1509×10^{7}	14.8

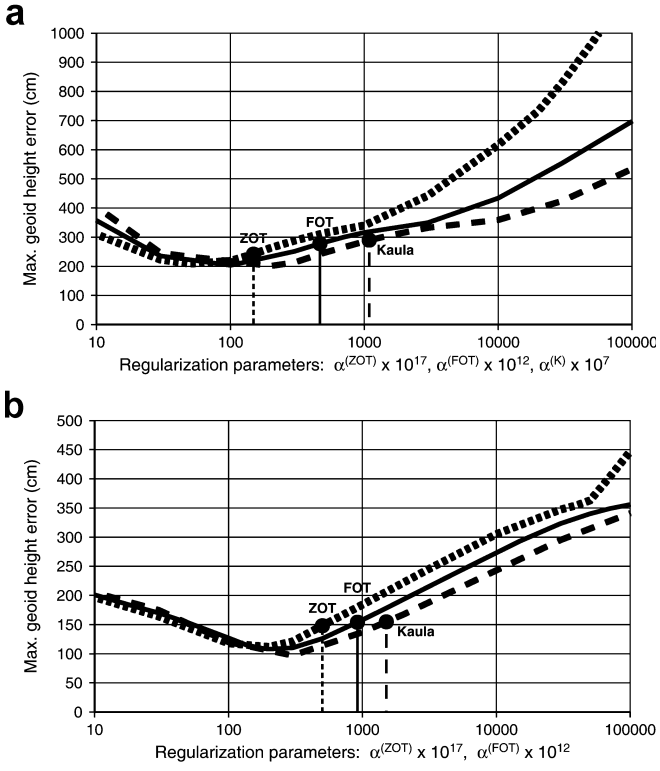

Fig. 10. Same as Fig. 9, but the maximum (in the absolute value) geoid height errors are considered instead of RMS errors

regularization parameters are preferable (Fig. 10). In fact, this is not surprising: by minimizing the maximum error, it is required that the propagated data noise is in balance with unrecovered high-frequency geoid variations not on average but in those areas where the variations are maximum.

Thus, it is not unreasonable to select a slightly smaller regularization parameter than the optimal one in the sense of the RMS geoid height error, so that maximum geoid height errors are also taken into account. From this point of view, solutions suggested in our experiments by the GCV method are probably not worse than those which could be selected manually on the basis of the known misfits with respect to the true model.

It is important to mention that the time expenditure required by the GCV method is not excessive. In our examples, 10–20 computations of the GCV function were performed each time to find the optimal regularization parameter; the required wall-clock time did not exceed 5 hours.

6 Discussion and conclusions

In the present paper, we have compared different regularization techniques and checked the behavior of the generalized cross-validation method for heuristic selection of the regularization parameter.

First of all, it was found that the exploitation of the ZOT or FOT regularization requires a precaution: the lowest degrees in the normal matrix should be excluded from the regularization, otherwise the obtained gravity field model is unacceptable. This conclusion is in agreement with that of Kusche and Klees (2002b), who observed erroneous gravity field models after a straightforward application of the ZOT regularization. As long as the above-mentioned precaution is introduced, all the considered regularization techniques lead to models of a very similar quality. A probable reason is that in all the cases the regularization plays a significant role in only a relatively narrow interval of highest degrees. Whichever regularization matrix is considered, elements of a regularization matrix do not vary significantly in such an interval. A very minor drawback of the ZOT regularization is an increased sensitivity to the right choice of the regularization parameter. As far as the numerical performance is concerned, the ZOT, the FOT, and the Kaula techniques require nearly the same number of PCCG iterations. An attempt to build a diagonal regularization matrix with elements growing faster than l^4 may, however, result in a dramatic increase in the number of PCCG iterations to be performed.

Satisfactory results we have obtained with the Kaula regularization disagree with the conclusions of Ditmar and Klees (2002), who claimed that the Kaula regularization may behave improperly in the SGG data processing when the maximum degree solved for is large. The reason for this mismatch, as was found recently, is a bug in the software used by Ditmar and Klees (2002).

Furthermore, we have assessed the generalized cross-validation method for heuristic selection of the regularization parameter. In all the examples considered, the

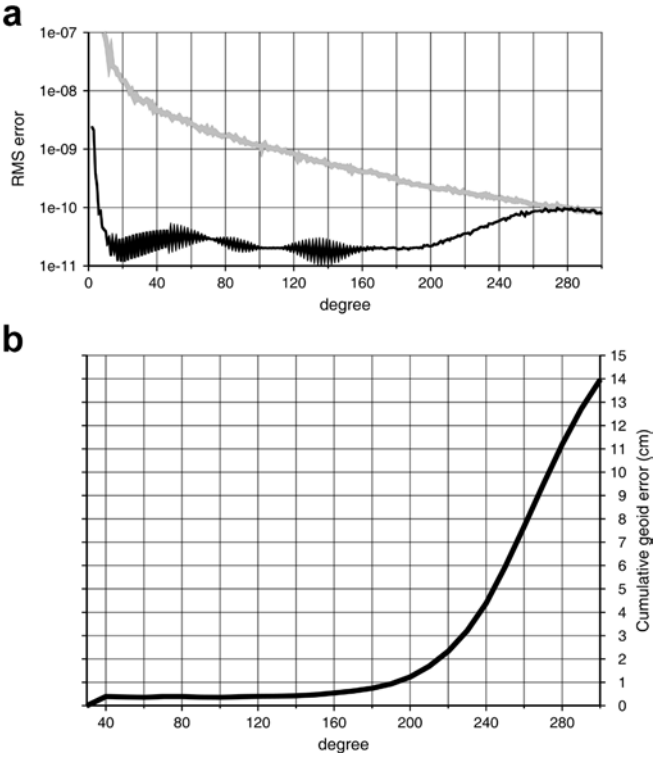

Fig. 11. Processing of the long data set with the FOT regularization; alternative ways to represent the results already shown in Fig. 4b. **a** Degree-error variances of the estimated spherical harmonic coefficients (*black line*) vs the OSU91a signal (*grey line*); **b** cumulative geoid height errors between degrees 31 and 300. Degrees below 31 are ignored because they cause unreasonably high errors; in practice these errors will be suppressed by taking satellite-to-satellite tracking data into account

choice offered by the GCV method proved to be very good. Importantly, the time expenditure required by the GCV method remained within reasonable limits (not more than 5 hours). Moreover, we expect that a proper software optimization will reduce this expenditure even further.

It is noteworthy that the optimal regularization parameter in case of the Kaula regularization was found to be 1.2×10^{10} for the short data set and 2×10^{10} for the long data set. These values are sufficiently close to the value prescribed by Kaula's rule of thumb: 10^{10}. It should be borne in mind, however, that the application of this rule requires a knowledge of noise in the data. If information about the noise level is absent, the covariance matrix in the objective function of Eq. (5) is known up to a certain constant factor. In this situation we cannot rely upon Kaula's rule of thumb or other previous estimations of the optimal regularization parameter, so that the exploitation of an heuristic parameter choice rule is almost indispensable.

So far, we have assessed the computed gravity field models only in terms of geoid height errors. In order to make an easier comparison of our results with those presented previously (see e.g. Bouman 2000; Sünkel 2000; Sneeuw 2002; Ditmar et al. 2003), we have also used two alternative representations of one of the best gravity field models obtained from the long data set (Fig. 4b): the degree-error variances of the estimated spherical harmonic coefficients (Fig. 11a) and the cumulative geoid height errors (Fig. 11b). From the latter figure, we can see, in particular, that the cumulative geoid height error at degree 200 is slightly above 1 cm. It is known, however, that the model accuracy improves with the square root of the number of data (provided that each new portion of data is not correlated with previous data). Hence we can conclude that processing of all the SGG data to be collected by the GOCE satellite will result in cumulative geoid height error at degree 200 of below 1 cm, which matches the mission requirements. However, we must be careful when using this square-root rule. This rule does not take regularization into account, whereas the application of a regularization can be treated as an extension of the data set to be considered. As can be seen from Fig. 11a, errors in the spherical harmonic coefficients at degrees above 280 are close to the coefficients themselves. This means that the solution at these degrees is fully controlled by the regularization. Increasing the number of data will barely reduce the errors in these coefficients. Therefore, we should not expect that a one-year data set would reduce the cumulative geoid error at degree 300 from 14 to 10 cm according to the square-root rule. A more realistic estimation is 12–13 cm. On the other hand, the fact that degrees above 280 are barely controlled by the data means that the corresponding geopotential coefficients which describe the disturbing potential will be close to zero. In other words, the model obtained after the data processing will not differ much from the reference one in the range of highest spatial frequencies. Therefore, the cumulative geoid height error at degree 300 is strongly dependent on the quality of the reference gravity field model. In our case, the GRS80 normal field, which is a most simple reference model, was used. Thus, our estimations should be considered as a worst-case scenario. In practice, the reference model will reflect the up-to-date knowledge of the Earth's gravity field, so that the cumulative geoid height error related to the degree 300 will be diminished.

It is noteworthy that we have considered in this paper only the SGG data processing alone. In practice, SGG data will be processed jointly with other types of observations, first of all with satellite-to-satellite tracking (SST) data. The SST data mostly control the range of lowest degrees. It is therefore likely that our precautions related to the ZOT and the FOT regularization will be not needed in such a joint processing. On the other hand, SST data are of no help in the range of highest degrees, where regularization plays the most significant role. Hence we believe that the other conclusions we have drawn will be valid in the case of the joint SST + SGG processing as well.

Acknowledgments. The authors thank Dr. E. Schrama for valuable discussions and for computing the orbit used to generate the long data set. They are also grateful to Prof. Tscherning and two anonymous reviewers for numerous valuable remarks and

suggestions. The orbit to generate the short data set was kindly provided by J. van den IJssel. Computing resources were provided by Stichting Nationale Computerfaciliteiten (NCF), grant SG-027.

References

Alenia (2001) Performance requirements and budgets for the gradiometric mission. Technical note *GO-TN-AI*-0027, Turin

Bertsekas DP (1982) Constrained optimization and Lagrange multiplier methods. Academic Press, New York

Bouman J (2000) Quality assessment of satellite-based global gravity field models. PhD Thesis, Delft University of Technology, Delft

Bouman R, Koop R (1998) Regularization in gradiometric analysis. Phys Chem Earth 23: 41–46

Colombo OL (1986) Notes on the mapping of the gravity field using satellite data. In: Sünkel H (ed) Mathematical and numerical techniques in physical geodesy. Lecture Notes in Earth Sciences, vol 7. Springer, Berlin, Heidelberg New York, pp 261–316

Ditmar P, Klees R (2002) A method to compute the Earth's gravity field from SGG/SST data to be acquired by the GOCE satellite. Delft University Press, Delft

Ditmar P, Klees R, Kostenko F (2003) Fast and accurate computation of spherical harmonic coefficients from satellite gravity-gradiometry data. J Geod 76: 690–705

European Space Agency (1999) Gravity field and steady-state ocean circulation missions. Reports for mission selection. The four candidate Earth explorer core missions, SP-1233(1). European Space Agency, Noordwijk

Girard DA (1989) A fast 'Monte-Carlo cross-validation' procedure for large least squares problems with noisy data. Numer Math 56: 1–23

Golub GH, Matt U (1997) Generalized cross-validation for large-scale problems. J Comput Graph Statist 6: 1–34

Golub GH, Wahba MHG (1979) Generalized cross-validation as a method for choosing a good ridge parameter. Technometrics 21: 215–223

Hestenes MR, Stiefel E (1952) Methods of conugate gradients for solving linear systems. J Res Nat Bur Stand 49: 409–436

Ilk KH (1993) Regularization for high resolution gravity field recovery by future satellite techniques. In: Angerer G, Gorenflo R, Moritz H, Webers W (eds) Inverse problems: principles and applications in geophysics, technology and medicine. Akademic Verlag, Berlin, pp 189–214

Kaula WM (1966) Theory of satellite geodesy. Blaisdell, Waltham, MA

Klees R, Broersen P (2002) How to handle colored noise in large least-squares problems. Building the optimal filter. Delft University Press, Delft

Klees R, Ditmar P, Broersen P (2003) How to handle colored observation noise in large-scale least-squares problems. J Geod 76: 629–640

Koch K-R, Kusche J (2002) Regularization of geopotential determination from satellite data by variance components. J Geod 76: 259–268

Koop R (1993) Global gravity field modeling using satellite gravity gradiometry. Publ Geodesy, New Series, Number 38. Nederlands Geodetic Comission, Delft

Kusche J, Klees R (2002a) On the regularization problem in gravity field determination from satellite gradiometric data. In: Adam J, Schwarz K-P (eds) Vistas for geodesy in the new millennium. International Association of Geodesy Symposia, vol 125. Springer, Berlin Heidelberg New York, pp 175–180

Kusche J, Klees R (2002b) Regularization of gravity field estimation from satellite gravity gradients. J Geod 76: 359–368

Kusche J, Mayer-Gürr T (2002) On the iterative solution of ill-conditioned normal equation by the use of Lanczos methods. In: Adam J, Schwarz K-P (eds) Vistas for geodesy in the new millennium. International Association of Geodesy Symposia, vol 125. Springer, Berlin Heidelberg New York, pp 248–252

Lonkhuyzen M, Klees R, Bouman J (2001) Regularization for the gravity field recovery from GOCE observations. In: Sideris MG (ed) Gravity, geoid and geodynamics 2000. International Association of Geodesy Symposia, vol 123. Springer, Berlin Heidelberg New York, pp 117–122

Meissl P (1971) A study of covariance functions related to the Earth's disturbing potential. Rep 151, Department of Geodetic Science and Surveying, The Ohio State University, Columbus

Moritz H (1980) Geodetic reference system 1980. Bull Géod 54: 395–405

Rapp R, Wang Y, Pavlis N (1991) The Ohio State 1991 geopotential and sea surface topography harmonic coefficient models. Rep 410, Department of Geodetic Science and Surveying, The Ohio State University, Columbus

Schuh WD (1996) Tailored numerical solution strategies for the global determination of the Earth's gravity filed. Folge 81, Mitteilungen der geodätischen Institute der Technischen Universität Graz, Graz

Sneeuw NJ (2002) Validation of fast pre-mission error analysis of the GOCE gradiometry mission by a full gravity field recovery simulation. J Geod 33: 43–52

Sünkel H (ed) (2000) From Eötvös to mGal. Final report, ESA/ESTEC Contract 13392/98/NL/GD. European Space Agency, Noordwijk

Tihonov AN (1963a) Regularization of incorrectly posed problems. Sov Math 4(6): 1624–1627

Tihonov AN (1963b) Solution of incorrectly formulated problems and the regularization method. Sov Math 4(4): 1035–1038

Tikhonov AN, Arsenin VY (1977) Solutions of ill-posed problems. VH Winston, Washington, DC

Wahba G (1990) Spline models for observational data. SIAM, Philadelphia, PA

Xu P (1992) Determination of surface gravity anomalies using gradiometric observables. Geophys J Int 110: 321–332